

September 4, 1987

Ms. Pauline P. Brooks  
Repository Projects Branch  
Division of Waste Management  
Office of Nuclear Material Safety and Safeguards  
United States Nuclear Regulatory Commission  
Washington, DC 20555

**RE: Contract NRC-02-81-026  
Benchmarking of Computer Codes and Licensing Assistance**


Dear Pauline:

Enclosed for your review are the results of the QC review of the work by GEO-TRANS. This review has been forwarded to GEO-TRANS for revision and incorporation into their document. I have been informed that the review will be completed in mid-October, at which time we will forward the final document to you.

I assume this may cause some problems at your end regarding the contract. I will contact you to discuss how this may be best resolved.

Please call with any questions.

Yours sincerely,



Charles J. Rosselle  
Vice President

CJR:rs  
Enclosure

8712140150 870904  
PDR WMRES EECCORS  
B-6985 PDR

88134327  
WM Projects WM-10, 11, 16  
PDR w/encl  
(Return to WM, 623-SS)

WM Record File: B-6985  
LPDR w/encl

H

**CorSTAR/TTS Project 6280  
Quality Control Review  
September 1, 1987**

**Benchmarking of Computer Codes  
Quality Control Review**

**Document Reviewed:**

**"Benchmarking of Flow and Transport Codes for Licensing Assistance", May 1987, GeoTrans, Inc.**

**Programs Reviewed:**

- 1. USGS3D**
- 2. PORFLO**
- 3. SWIFT**

**General Comments.**

The documentation, as presented in the GeoTrans report, of the results of benchmark testing of the three programs mentioned above, was reviewed. The comments made on each of the test problems that were run, fall into the following categories:

- 1. Comments on the formulation of the test problem and its ability to meet the general objectives as stated in "Benchmarking Problems for Repository Siting Models" (NUREG/CR-3097, 1982).**
- 2. Comments on the discussion of the accuracy of results and comparisons with other presented solutions.**
- 3. Comments of an editorial nature, including apparent typographical errors or inconsistencies in cross-referencing noted in the text or in the Tables and Figures.**

In general, the organization and presentation of the problems and results are well made. The theoretical background and problem formulation are adequately and completely presented with appropriate references provided.

In the introductory section of the report, there are some inconsistencies between the codes and problems listed in Table 1.1, the actual benchmark problems reported, and the table of contents. For example, PORFLO problem 5.3 was not solved, and CCC problems 5.2 and 5.3 do not appear in the table of contents. Table 1.1 needs to be revised to reflect the set of problems actually solved.

Comments on Program USGS3D

Problem 3.2 -- TRANSIENT RADIAL FLOW TO A FULLY PENETRATING WELL IN A LEAKY AQUIFER SYSTEM.

1. The theoretical development of the problem is adequately presented.
2. Model discretization is appropriate. Considerations of contrast in discretization at layer interface, different discretizations for short-term and long-term solution, use of 'adjusted time' scale for long-term solution which ignores the effect of storage in the aquitard, were found to be adequately treated.
3. The physical parameters chosen (on p. 16) are not the ones suggested in NUREG/CR-3097, and no explanation for the variance is given. Many of the parameters chosen, such as aquitard thickness, hydraulic conductivity of the aquitard, well discharge Q, and distance at which drawdown is computed, are different from the values suggested in the NUREG. An explanation should be provided.
4. If conforming to the NUREG values was not essential for the benchmark, a test problem with  $r = 100m$ , and time steps in multiples of 125 sec (with other parameters the same as run), would have been a very convenient case to run, since it can be compared with  $H(u,B)$  values taken directly from Hantush(1960), without any interpolation.
5. The time intervals for computation (on p. 19) do not agree with those recorded in Tables 2.1a and 2.1b. The differences should be reconciled.
6. Equation at the bottom of p. 14 should read:

$$u' = ( 1 + S'/3S ) u$$

Problem 3.3 -- FLOW TO A FULLY PENETRATING WELL IN AN ANISOTROPIC CONFINED AQUIFER.

1. The problem discretization, both spatially and temporally, appears adequate. Results for drawdown versus time compare well with analytical solution.
2. The example problem considers the special case of anisotropic transmissivity along principal axes i.e. with  $T_{xy} = 0$ . A more

- general benchmark test of the program would have been to run a case with  $T_{xy} > 0$ , provided the program has this capability.
3. The drawdown distribution along X and Y axes (Fig. 2.6, and Table 2.3) appear reasonable. However, analytical values using well function tables could have been calculated to obtain a more convincing quantitative comparison.
  4. In Table 2.3 the value of drawdown at  $x = 100$  m, given as 6.01 m should be reconciled with the corresponding result given in Table 2.2 which is 6.10 m. (One of these values is presumably a typographical error).

**Problem 3.4 -- AREAL FLOW IN MUSQUODOBOIT RIVER BASIN.**

1. The spatial and temporal discretization appear to be adequate, and the results are in generally good agreement.
2. In Fig. 2.13, comparison with field data appears much too cluttered because numerous analysis results are superimposed, and graphical symbols used are all very similar. It is suggested that only a comparison of USGS3D results and field data be presented in this figure, and a separate figure be used to USGS3D compare results with SWIFT results.
3. The variations between computed and field data seem larger in the initial periods. An explanation or comment on this should be included in the discussion of results.
4. In Fig. 2.15, the results computed with and without river discharge cannot be distinguished clearly because of the similarity of plot symbols.

**Problem 3.5 -- THREE-DIMENSIONAL FLOW IN A HYPOTHETICAL BASALT REPOSITORY.**

1. In describing the discretization data there is no mention of approximating the hypothetical basin, including inclined aquifers, by an orthogonal block or grid. If the approximation is considered not significant to the benchmarking, this should be stated.
2. For discussion of results with reference to Fig. 2.21 and 2.22, it would help the reader if some frame of reference was provided on the figures. Suggestions are to superimpose the coordinate axes, show a North arrow, and possibly indicate the boundaries that correspond to the crush zone, the recharge area, and the river.

Comments on Program PORFLO

Problem 3.2 -- FLOW TO WELL IN A LEAKY AQUIFER SYSTEM.

1. In Fig. 3.1, providing only the results from PORFLO compared with the analytical solution would allow an uncluttered comparison, and would be consistent with the discussion in paragraph 3.2.3.

Problem 3.3 -- FULLY PENETRATING WELL IN A HORIZONTAL ANISOTROPIC AQUIFER.

1. The discussion of results (section 3.3.3) compares PORFLO results with USGS3D results. First, it is unnecessary to compare Fig. 3.2 with Fig. 2.5, since both PORFLO and USGS3D results are shown in Fig. 3.2 itself. Second, the explanation for the poorer accuracy of PORFLO, based on the differences in time-stepping techniques, appears to be the predominant factor. However, the approximation involved in running PORFLO with equivalent isotropic transmissivity (using the geometric mean of the orthogonal transmissivities), and adjusting time scale factors to present "equivalent anisotropic" results should be noted as an additional factor in the comparison of accuracy.
2. Fig. 3.2 should be moved to follow the discussion of results of problem 3.3, i.e., after p. 61.

Problem 5.1a -- RADIAL HEAT TRANSPORT DURING WELL INJECTION.

1. For this problem, both the radial grid refinement and the two different vertical grid refinements for the case with and without boundary thermal conduction, were selected to obtain good agreement with the analytical solutions. It was also demonstrated by comparison with analytical solution that the time discretization was adequate to get stable solutions.
2. Fig. 3.4 and Fig. 3.5 show results obtained using program CCC in addition to PORFLO results and analytical solutions. However, no discussion or comparison with CCC results are made. Such comparisons would have been helpful, particularly with respect to relative time intervals and computer run times required to obtain the more accurate solutions with CCC. If these discussions are deferred to the section of the report on CCC (which we are not reviewing), then the Figs. 3.4 and 3.5 need not show the CCC results.

**Problem 5.1b -- LINEAR HEAT TRANSPORT DURING INJECTION.**

1. There is no discussion of the CCC results presented in Fig. 3.7 and Fig. 3.8 . It might, therefore, be best to eliminate these results from these figures so that the four PORFLO cases can be compared without the additional clutter.
2. In explaining the accuracy of solutions for the various cases shown in Fig. 3.8, there may be some inconsistencies in the discussion in Section 3.5.3 (on p. 77a). Firstly, it is not clear that the disagreement for case 1 is generally greater than case 2. Secondly, the explanation for the disagreement for case 1 is not consistent with the previous discussion of the radial heat transport results, shown in Fig. 3.7, in which an explanation is provided for case 1 results (with heat conduction) being better simulated by the program.
3. The equation for initial condition, Eq. (3.8b) on p. 72 should be corrected to:  $u(0,0,t) = 1$  .
4. Equations (3.10b) and (3.10c) on p. 74a were in draft form. These need to be checked and finalized.
5. All the figures and tables in this section should refer to problem 5.1b and not 5.1a as shown at present.
6. Fig. 3.9 does not belong to this problem. This figure is a duplicate of Fig. 3.5, which belongs to problem 5.1a. The figure and reference to it on p. 79a, second para, should be deleted.
7. In Table 3.10 the vertical discretization should be shown as z-coordinates to be consistent with Table 3.5 and the discussion of the problem statement in Section 3.5.1 .

**Problem 5.2 -- HEAT TRANSPORT BETWEEN INJECTION AND WITHDRAWAL WELLS.**

1. It appears from the assumptions and limitations stated in Section 3.6.4 , that the benchmark problem 5.2 is not a suitable problem to test the capabilities of PORFLO, or conversely PORFLO does not have the capabilities to meet the objectives as given in NUREG/CR-3097 for solving problem 5.2 . The reasons for this are:
  - a. The problem needs a three-dimensional simulation, but the

program is restricted to two-dimensional for the heat conduction effect.

- b. The zero-conductivity boundary within the aquifer has to be approximated by a small value in PORFLO.
  - c. Only one of four cases suggested by the NUREG could be simulated, and even this was only an approximate match for the case of  $L = 300$ .
  - d. The PORFLO solution scheme is unable to predict stable results using time-steps which are computationally feasible. It is suggested that an explicit concluding statement be inserted in the discussion of results in Section 3.6.4 that this problem is unsuitable for PORFLO.
2. In Section 3.6.3, the discussion of grid representation uses the phrase "upper half of the flow region". This suggests a vertical division and is thus slightly confusing. It might be better to say "one half of the flow region" in this paragraph and in the title of Fig. 3.12.
  3. Fig. 3.13 does not show the analytical curve for the case of infinite  $\lambda$ -D, and therefore the discussion in Section 3.6.3, second paragraph, is not consistent with the presented data. Either the figure or the discussion should be revised.
  4. In Table 3.13 the units for "Specific volume heat capacity" should be:  $\text{BTU}/(\text{ft}^3 \cdot ^\circ\text{F})$ .
  5. Some corrections on page 81 are marked on the attached copy of this sheet.

**Problem 8.1 -- ONE-DIMENSIONAL RADIONUCLIDE MIGRATION WITH CHAIN DECAY AND CONSTANT MIGRATION FACTORS.**

1. It is noted that for this problem results are presented with only a brief discussion. It would be helpful to provide some elaboration on the comparison of these results with analytical results and/or results using other codes.
2. Some discussion or recommendation on the application of this code for problems of this nature should be provided, citing the advantages of using this code for a specific application despite its limitations; for example, obtaining approximate breakthrough

curves for the slowest decaying component at comparatively low computational cost.

3. In Tables 3.19a through 3.19h, there is inconsistency in the exponent of C MAX values as compared with the maximum values in Table 3.18.
4. In Tables 3.19a through 3.19h it would be helpful to clarify that the BENCHMARK CASE: 1 referred to is an INTRACON case.

**Problem 8.2 -- TWO-DIMENSIONAL RADIONUCLIDE MIGRATION WITH CHAIN DECAY.**

1. In Section 3.8.2, the discussion of grid representation uses the phrase "upper half of the flow region". This suggests a vertical division and is thus slightly confusing. It might be better to say "one half of the flow region" in this paragraph and in the title of Fig. 3.18, and Table 3.22.
2. The left hand side of Equation (3.22b) should be  $F_r(0,t)$ , similar to Eq. (3.18b) in Problem 8.1.
3. There is an inconsistency in the units for Concentration between Fig. 3.20 and Table 3.23.
4. There are no other substantive comments on this problem. The development of the problem, model parameters used in PORFLO, and comparison of results appear satisfactory.

**Problem 8.3 -- ONE-DIMENSIONAL RADIONUCLIDE MIGRATION WITH CHAIN DECAY.**

1. The formulation of this problem on PORFLO with spatial discretization as selected, and the two different temporal discretizations for the two cases with differing retardation factors, gives generally satisfactory predictions for breakthrough curves.
2. It would be informative to mention in Section 3.9.3 that PORFLO predicts a lower value for time of occurrence of peak concentration compared to other codes.
3. Can an explanation be offered for the better match for case 1 than for case 2, using PORFLO ?
4. In Tables 3.26a and 3.26b, it would be helpful to clarify that the BENCHMARK CASE: 2 referred to is an INTRACON case.



CorSTAR/TTS Project 6280  
Quality Control Review  
September 1, 1987

**Problem 9.1 -- ONE-DIMENSIONAL ADVECTION-DISPERSION IN A FRACTURED POROUS MEDIA.**

No comments. It appears from the simulation results obtained that the PORFLO code is not suitable for this problem.

**CorSTAR/TTS Project 6280  
Quality Control Review  
September 1, 1987**

**Comments on Program SWIFT**

**Problem 3.2 -- FLOW TO A WELL IN A LEAKY AQUIFER SYSTEM.**

1. Given the choice of aquifer boundary at a large radius compared to the distance of observation, the effect on the results of the Carter-Tracy option is probably minimal. Was any attempt made to observe the effect of this boundary by applying it at a smaller radius ?
2. Fig. 4.2 appears very cluttered with results from numerous programs superimposed. It would be helpful to present results for only the SWIFT code for comparison with the analytical results.

**Problem 3.4 -- AREAL FLOW IN MUSQUODOBOIT RIVER BASIN.**

1. Spatial and temporal discretization appear adequate for comparable accuracy of results with USGS3D results.
2. Fig. 4.4 displays too much data to permit distinguishing between results obtained by the different programs and cases. See also comment no. 2 on USGS3D Problem 3.4.
3. In the discussion of the results some explanation should be added for the not-so-good correlation with the reference solution during the first 100 minutes.
4. Can any general conclusion be drawn regarding the overprediction of drawdown by both USGS3D and SWIFT, particularly SWIFT, for wells 1 and 2, as seen in Fig. 4.5. ?

**Problem 3.5 -- THREE-DIMENSIONAL FLOW NEAR A HYPOTHETICAL BASALT REPOSITORY.**

1. Section 4.4.1 and 4.4.2 should refer back to Section 2.5 (not 2.4).
2. Some comment should be provided on approximating inclined aquifers by vertical layers in the simulation grid. See also comment no. 1 on USGS3D Problem 3.5.
3. Contour plots of hydraulic head (Figs. 4.6 and 4.7) agree generally well with those obtained from USGS3D. Can these be plotted to identical scales so that they might be superimposed for comparison?

**CorSTAR/TTS Project 6280**  
**Quality Control Review**  
**September 1, 1987**

4. Some reference axes should be provided on Figs. 4.6 and 4.7 to help orient the reader. See comment no. 2 on USGS3D Problem 3.5.

**Problem 3.6 -- TWO-DIMENSIONAL FLOW NEAR A HYPOTHETICAL BEDDED SALT REPOSITORY.**

1. Model spatial discretization (250m horizontal by 50m vertical) seem adequate and consistent with other problems solved by SWIFT.
2. For this problem no comparable results from other programs were available. Any validation checks that were performed to increase the confidence in the results should be discussed in Section 4.5.4.

**Problem 5.2 -- HEAT TANSPORT BETWEEN INJECTION AND WITHDRAWAL WELLS.**

1. In the discussion of simulation results (Section 4.6.4), it would be helpful, if possible, to give some quantitative comparisons between SWIFT results and those of the analytical solution.
2. A qualitative discussion of the relative effort involved in data preparation for the rectangular and curvilinear models e.g. precalculation of pore volumes for each grid block for SWIFT, may be helpful in emphasizing the effort required to get more accurate results using the curvilinear model.
3. On Fig. 4.17, the quantities "Dimensionless Temperature" and "Dimensionless Time" are not defined in the related section. Either the definitions should be provided, or reference should be made to Fig. 3.11 which is for PORFLO Problem 5.2.
4. Some typographical corrections on pages 174 and 175 are marked on attached copies of these sheets.

**Problem 5.3 -- FLOW AND HEAT TRANSPORT INDUCED BY A DECAYING SOURCE IN A HYPOTHETICAL BASALT REPOSITORY.**

1. For this problem, taking a two-dimensional approach may be a good engineering solution but does not meet the objectives of this benchmark problem, as stated in NUREG/CR-3097, to exercise all segments of the code logic needed to simulate buoyancy induced three-dimensional transient and fluid flow.
2. In Section 4.7.3, the discussion of the validity of the 2-D approach states that at 1000 years the repository is 10°C higher. A more realistic measure of the accuracy might have been obtained by

**CorSTAR/TTS Project 6280**  
**Quality Control Review**  
**September 1, 1987**

stating that the difference was 10°C in a total of 80°C, or 12.5%.

3. For temperature contours shown on p. 199-201, comparisons with other programs e.g. CCC, should have been provided, if possible, to validate the accuracy of SWIFT, and the 2-D assumption along a selected inclined plane. Similarly, Darcy velocities should also have been compared to satisfy the output requirements in the NUREG.
4. In Table 4.23, the value for thermal conductivity for Aquifers 1 and 2, are not in agreement with that specified in NUREG/CR-3097, p. 70, but appears to be the more reasonable value. Please verify.
5. On p. 197, the discussion on the time after which the velocities near the repository begin to decrease should be 1 year rather than 10 years, referring to Fig. 4.24 for locations A and B.
6. Some typographical corrections on p. 186 are marked on the attached copy.
7. In Fig. 4.24, the logarithmic scale markings along the two unlabeled edges of the figure are on a reciprocal scale compared to the Time and Velocity axes. This is probably unintended.

**Problem 7.1 -- COUPLED FLUID FLOW, SOLUTE TRANSPORT, AND HEAT TRANSPORT  
NEAR A HYPOTHETICAL BEDDED-SALT REPOSITORY.**

1. Discussion of simulation of results in Section 4.8.4 on p. 212 provides a qualitative result for the distribution of overall salinity during the 1000-yr period. Since the output specification for Problem 7.1 (NUREG/CR-3097, p. 86), requires salt concentration as a function of time at six specific locations, a more quantitative result would have been appropriate.
2. The NUREG requires two components of ground velocity at six locations as a function of time. The results presented in Table 4.33 are for only the vertical component of velocity for locations A and E. For the other components and locations, either the computed results should have been presented, or some explanation for not presenting this information should have been given.
3. It is noted that for this problem the results are not compared with any other solution, nor is any discussion provided on the accuracy of the results. Can some comparisons or discussion be provided in the text to increase confidence in these results ?

4. In Table 4.28, should the value for Thermal Conductivity of the Rubble Zone have been  $20 \text{ W/(m}^\circ\text{C)}$ , as given on p. 73 of the NUREG? What value was actually used in SWIFT?
5. Some typographical corrections on pages 207, 211, and 212, are shown on attached copies of these sheets.

**Problem 8.2 -- TWO-DIMENSIONAL RADIONUCLIDE MIGRATION WITH CHAIN DECAY AND CONSTANT RETARDATION FACTORS AND DISPERSIVITY**

1. Selection of boundaries of the model at  $x = x_1$  and  $y = y_1$  does not have any supporting material to show that the target line concentrations are not influenced. Parametric studies or other arguments that were used to justify the selection of these boundary positions should be presented.
2. The discussion of simulation results notes, correctly, that use of curvilinear simulation is advantageous with respect to computer efficiency. It might be informative to mention, however, that the effort of input preparation e.g. calculation of pore volumes, is somewhat more for this case.
3. For results in the form of release rates across the target line, it should be mentioned that twice the tabular values (Table 4.40), should be used for comparison, since symmetry about the x-axis was employed. Also, reference should be made to comparison of results with other codes e.g. NUTRAN.
4. Some typographical corrections on pages 216, 220, 222, 224, 228, 229, and 230 are shown on attached copies of these sheets.
5. Tables 4.40 through 4.48 which present results, appear to be copies of pages from some other report, and therefore need to be given correct Table numbers and paginated. Copies of these pages are attached.

**Problem 8.4 -- TRANSPORT OF A THREE-MEMBER CHAIN OF RADIONUCLIDES FROM A HYPOTHETICAL BASALT REPOSITORY**

1. It was assumed, for this problem solution, that the radionuclide transport is one-dimensional following the basic streamline and neglecting lateral dispersion. Regardless of the accuracy of this assumption, the objective of this benchmark problem as stated in NUREG/CR-3097 was to test the capacity of the code to simulate

**CorSTAR/TTS Project 6280**  
**Quality Control Review**  
**September 1, 1987**

transport in a three-dimensional flow field. By reducing the problem to considering only one streamline, the capacity of the program to simulate three-dimensional transport is not checked.

2. In the streamline considered only Aquifer 1 is contaminated as seen in Fig. 4.32, but the NUREG (p. 70 and p. 97) requires that changes be made to parameters to ensure that both aquifers are contaminated.
3. The results have not been compared with those of other programs, and therefore the accuracy of the predictions are not evident.
4. Since only a single streamline has been considered, the discharge rate per unit length along the river as a function of position cannot be given, though this was required by the NUREG output specification (p. 97). Some explanation for not addressing the objectives stated in the NUREG should be provided.
5. On p. 236, transverse dispersion is assumed to be 10 percent of longitudinal. However, for SWIFT Problem 5.3, in Table 4.23 a value of 20 percent is used for transverse. Do these two cases need to be consistent?
6. In Table 4.49, the Retardation factors for Basalt are all given as
  1. Based on NUREG/CR-3097, p. 96, and Table A-2 on p.134, Retardation Factors for Basalt should be 300 for  $^{234}\text{U}$ , 20,000 for  $^{230}\text{Th}$ , and 10,000 for  $^{226}\text{Ra}$ . What values were actually used in SWIFT ?
7. Some typographical corrections on pages 233, 235, and 236 are marked on attached copies of these sheets.

**CorSTAR/TTS Project 6280  
Quality Control Review  
September 1, 1987**

**ATTACHMENT**

**COPIES OF GEOTRANS REPORT PAGES MARKED  
WITH TYPOGRAPHICAL CORRECTIONS**

previously.

The initial and boundary conditions may be represented by

$$T(x,y,z,0) = T_0 \quad (3.13a)$$

$$T(0,0,z,t) = T_1 \quad (3.13b)$$

$$\lim_{x^2 + y^2 + z^2 \rightarrow \infty} T(x,y,z,t) = T_0 \quad (3.13c)$$

A semianalytical solution of the above problem was developed by Gringarten and Sauty (1975). The solution was derived based on an assumption of pure convection in the aquifer (i.e.,  $K_m = 0$ ). The general expression for ~~temperature distribution in the aquifer~~ is given by

$$\frac{T_0 - T_w}{T_0 - T_1} \int \operatorname{erfc} \left\{ \frac{d(S_{max}/D^2)}{d(\psi/Q)} \left[ \lambda(t_D - \frac{d(S_{max}/D^2)}{d(\psi/Q)}) \right]^{-1} \right\} d(\frac{\psi}{Q}) \quad (3.14)$$

where

$$u = (T - T_0)/(T_1 - T_0);$$

$S_{max}$  = the total stream channel area between the two wells;

$\psi$  = stream line function;

$D$  = a characteristic length; and

$t_D$  = dimensionless time.

The expression for temperature at the pumped well ( $T_w$ ) may be written in the following functional form:

$$(T_0 - T_w)/(T_0 - T_1) = T_D(t_D, \lambda_D) \quad (3.15)$$

where  $T_D$  is a dimensionless function and  $t_D$  and  $\lambda_D$  are dimensionless parameters defined as

$$t_D = \frac{\rho_w c_w Q t}{\rho_m c_m D^2 b} \quad (3.16a)$$

$$\lambda_D = \frac{\rho_w c_w \rho_m c_m Q b}{D^2 K_R \rho_R c_R} \quad (3.16b)$$



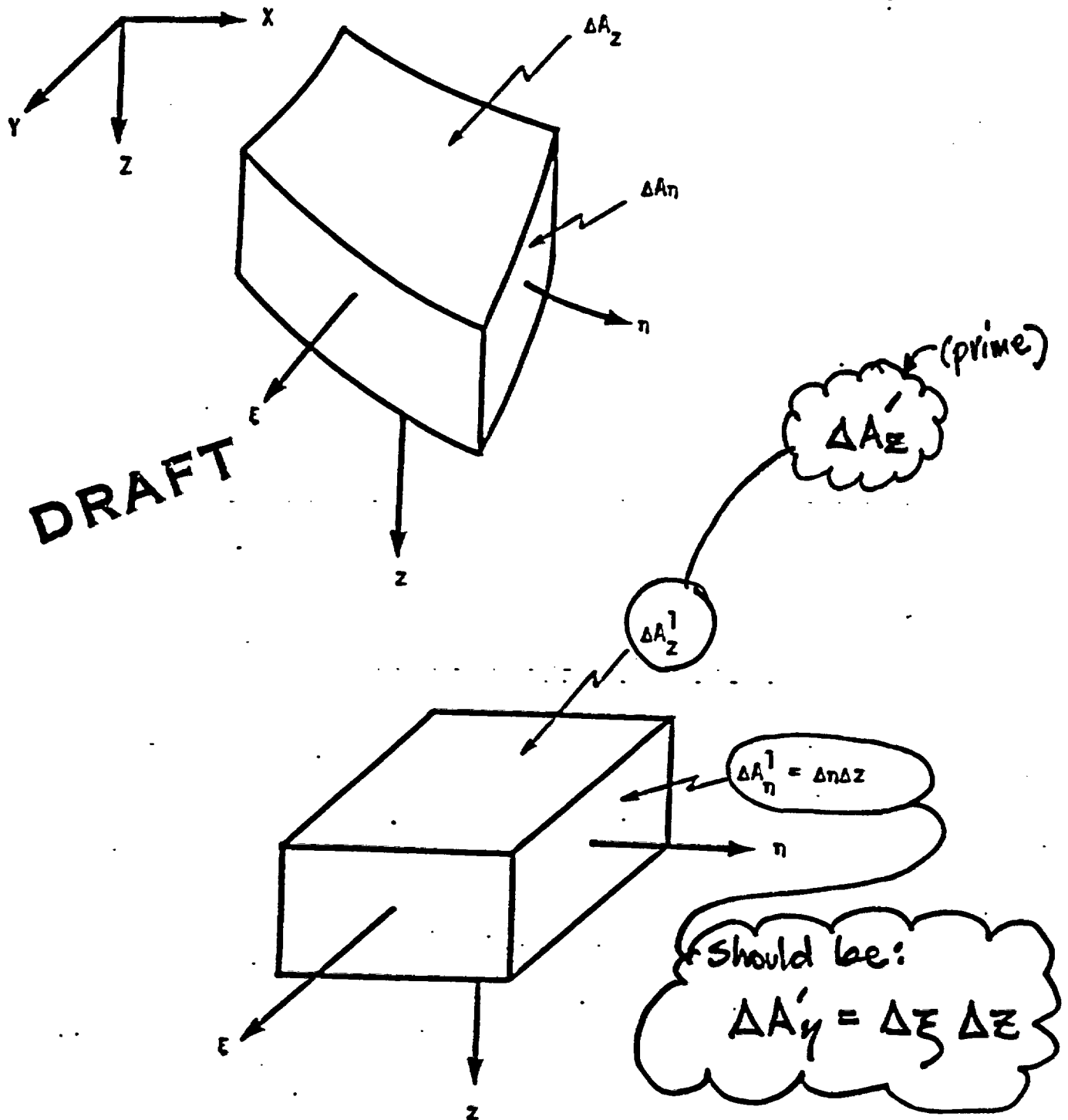


Figure 4.15. Schematic drawings of typical grid blocks in Cartesian and curvilinear geometries for use with SWIFT and problem 5.2.

Here  $\epsilon$  is the porosity, and the quantities  $h$  are the scale factors

$$h_\eta = h_\xi = x_1 / [(\cos(\eta) - \cos(\xi))] \quad (4.16)$$

(See the discussion of Margenau and Murphy (1956) on bipolar coordinates for a derivation of these scale factors.) Table 4.17 contains the pore volume of each grid block. These values were precalculated using equations (4.14 and 4.15) and then inserted directly into the code.

Fluid flow  $U$  is calculated by the code. It is directed along a streamline and is constant for a given stream tube  $\Delta\xi_j$ . Darcy flux is obtained for the output and for the calculation of dispersion. It should be determined as follows:

$$u_\eta = U_\eta / \Delta A_\eta \quad (4.17)$$

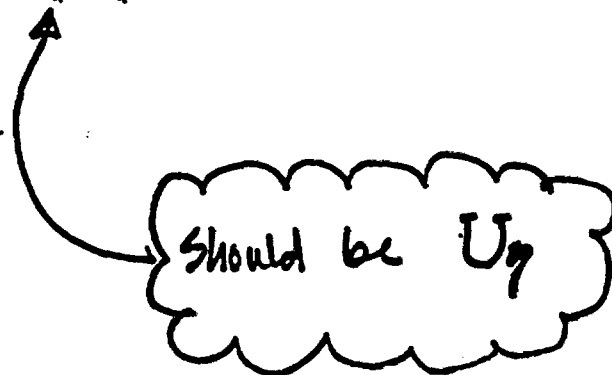
where  $\Delta A_\eta$  is the side area of the block shown in Figure 4.15. This area is given by

$$\Delta A_\eta = \Delta z \int h_\xi d\xi \quad (4.18)$$

where the integral is directed along the line  $\eta = \eta_{i+\frac{1}{2}}$ .

Actually, because of the grid which was set up initially, the Darcy flux is calculated via

$$u'_\eta = U_\eta / \Delta z \Delta \xi = u_\eta / \Delta A'_\eta \quad (4.19)$$



#### 4.7 PROBLEM 5.3: FLOW AND ASSOCIATED HEAT TRANSPORT INDUCED BY A DECAYING SOURCE IN A HYPOTHETICAL BASALT REPOSITORY

##### 4.7.1 Problem Statement and Objectives

The physical system is the same as that of problem 3.5 and is described in Section 2.5. There are several important units of the flow system, all of which are shown in Figures 2.18 through 2.20. They include two aquifers separated by an aquitard, zones of recharge and high permeability caused by the uplift of ridges, an ancient river bed, and a river. *2.16 through 2.18*

Here it is assumed that a repository (as shown in Figures 4.18 and 4.19) provides a heat source for the surrounding formation. The scale for heat transport is much more localized than it was for the *flow* ~~blow~~. As such, the important units in this case are the aquitard, in which the repository is placed, the aquifers, and the (assumed) over/underburden zones.

The objective is twofold:

- o to determine temperature contours, in vertical cross-section, for the times  $t = 10, 100, \text{ and } 1000 \text{ yr}$ , and
- o to determine Darcy velocities at the four points shown in Figure 4.20.

##### 4.7.2 Input Specifications

Initially the temperature is assumed to be uniformly constant  $T = 20^\circ\text{C}$  over the entire system. The thermal loading values given in Table 4.22 provide the heat source with the thermal properties of Table 4.23, determining the heat transport. The hydraulic conductivity is provided in Table 2.2. Water dependent properties are provided in Table 4.24.

*There appears to be an error in this reference.*

For the second step, the system was observed (via computer simulation) as it evolved transiently under the influence of the thermal source. Here, both the Darcy velocity at the repository and the rate of dissolution of the intact salt bed are of interest. The latter, of course, is controlled by diffusion and is of importance in analyzing the stability of the remaining portion of the salt bed.

Discretization. Spatially, the disturbed system was simulated with the same 28 x 20 grid as that used for the undisturbed system (see Figure 4.11). Temporally, the grid of Table 4.31 was employed. Backward differencing was applied in both space and time domains.

#### 4.8.4 Simulation Results

To implement the first part of the two-step procedure discussed above, a steady-state solution for coupled flow and brine transport was obtained for the disturbed system. The flow rates obtained for the sandstones were not significantly different from those of the undisturbed system (Figure 4.12). However, for the rubble zone, the flows generally exhibited a U-tube structure as shown by the stream lines of Figure 4.25. At Position E, within the repository, the Darcy velocity was directed upward rather than downward as in the undisturbed case, with a magnitude three times greater than for the undisturbed case. The concentration isopleths (Figure 4.25) were focused about the two intact zones of the salt, as expected. However, the concentration at the river did show a decrease of 21 percent relative to that of the undisturbed system. Perhaps the most significant effect of the rubble zone was a decrease in travel time. For the undisturbed case over 200 million years was required for a fluid particle to travel from repository to river. After rubblization time required, although variable, was decreased substantially. Travel times ranged from one to 50 thousand years depending on the point of release (Table 4.32). (See Table 4.31 and Figure 4.25 for added specificity.)

To implement the second step, heat loading was added to the repository. Then a transient pressure, heat and brine-transport calculation was performed using the step one steady-state result as an

Should be  
Figure 4.27?

Table 4.32. Fluid-particle travel times from repository to river calculated using SWIFT for problem 7.1.

Streamline*	Travel Time (yr)
A	5140
B	1740
C	1205
D	6180
E	1230
F	47410
G	5200
H	5260
I	4690
J	5010

\* See Figure 4.23<sup>23</sup> for specification of the streamlines.

\* See Figure 4.23 for specification of the stream lines.

should be Figure 4.25?

Should be 4.26?

initial condition on the system. Figure 4.27 shows the growth of one isotherm as a function of time. At the earlier times, the isotherm is symmetric, indicating the dominant role of thermal conduction through the rock. At the later times, however, the isotherm shows some convection in that its shape is modified by the flow field within the rubble zone. The U-shape of the flow field is maintained through the transient response to the change in temperature and is basically the same as that shown in Figure 4.27. However, the magnitudes of the Darcy velocity at Positions A and E within the repository do vary with time as given in Table 4.33. The velocity at point E is increased as a result of the heat, sometimes by as much as a factor of two.

Should be 4.25?

The thermal loading in the repository produces little change in the overall salinity distribution during the 1000-year time period (Figure 4.27). In contrast to the undisturbed system, there is approximately 30 percent less salt available for dissolution (38 versus 54 blocks, 250 m x 50 m) because of the presence of the rubble zone. In the disturbed system (with the rubble zone), the steady-state dissolution rate is only 21.3 percent less. In other words, for the case where rubble zone is included, although additional area is available for dissolution, the total rate of salt dissolution is less. This is expected because the steady-state rate of dissolution for this problem is strongly related to the molecular diffusion and concentration gradients in the vicinity of the salt. This observation is also true for the transient results. The variation in the rate of dissolution in the presence of the thermal load was calculated to be less than one percent.

The discharge of saline water to the river was not found to vary significantly from the steady-state rate (Figure 4.28). The rate did decrease to a minimum rate after approximately 600 years. The effect is a delayed response of the thermal plume rising in the rubble zone. After one thousand years the thermal gradients have dissipated significantly, thus velocities and brine discharge rates begin to return slowly to steady-state values.

#### 4.9 PROBLEM 8.2: TWO-DIMENSIONAL RADIONUCLIDE MIGRATION BETWEEN INJECTION AND WITHDRAWAL WELLS WITH CHAIN DECAY AND CONSTANT RETARDATION FACTORS AND DISPERSIVITY

##### 4.9.1 Problem Statement and Objectives

This problem, which is also known as INTRACON Case 4b (INTRACON, 1984), is defined in Section 3.6.

##### 4.9.2 Input Specifications

Table 3.14 of Section 3.6 provides geometrical and transport parameters. Table 3.10 of Section 3.6 specifies the radionuclide inventory  $I_1$  and the retardation set  $R_2$  which are to be used.

Table 3.20 of Section 3.8

Table 3.16 of Section 3.7

##### 4.9.3 Discretization Data

Because of the nature of the doublet flow field, a finite-difference solution of the radionuclide transport on a rectangular Cartesian grid may exhibit grid-orientation effects. This is a numerical dispersion lateral to the flow lines attributable to the orientation of the grid. Consequently, the decision was made here to use both Cartesian and natural, curvilinear coordinates. The latter take the actual potential contours and streamlines of the doublet flow field as coordinate axes and, as such, cause no grid-orientation effects. As an added benefit, simulation in both systems of coordinates provided an excellent demonstration efficiency of curvilinear coordinates as compared to Cartesian coordinates.

Cartesian Grids. The partial system shown in Figure 4.29 was chosen for the simulation in a Cartesian geometry. The two lines of symmetry would permit solution of only one fourth of the two-well flow system. However, the objective is to determine radionuclide transport and, more specifically, to characterize breakthrough at the target line  $x = 0$ . A half-system boundary  $x = \bar{x}_1$  shown in Figure 4.29 was placed at a sufficient distance to the right of the centerline that the convective boundary condition

$$\frac{dC_r}{dx} (x=\bar{x}_1) = 0 \quad (4.24)$$

would not perturb the target-line concentrations  $C_r$ . The two

were reproduced by the numeric flow field to within a few percent. Secondly, the mesh in the x direction between source and target lines was constructed in such a manner that the analytic source-to-target travel time for the streamline  $y = 0$  was reproduced to within a few tenths of a percent. Thirdly, the remaining grid in the y direction was fixed so as to characterize the source streamtube and neighboring streamtubes which might reasonably be expected to carry laterally dispersed constituents to the target line during the time period to be considered.

The time grid was established by considering grid-block throughput times for the most direct streamline along the line  $y = 0$ . Within the time regime that radionuclide fronts are within the near vicinity of the source, throughput travel times are relatively short and backward-in-time (BIT) differencing is the least restrictive (see Reeves et al., 1986b). For the time regime during which radionuclide fronts are a sufficient distance from the source (and the injection well), throughput times are relatively long, and centered-in-time (CIT) differencing is the least restrictive. Based on these considerations the temporal grid of Table 4.35 was adopted.

Curvilinear Grids. The partial system shown in Figure 4.30a was chosen for the simulation in a curvilinear geometry. As shown, the system is confined to the region

$$-4.84 \leq \eta \leq 0.697, \quad 1.04 \leq \xi \leq \pi$$

(4.27)

For the dimensionless potential coordinate  $\eta$ , the lower bound  $\bar{\eta}_0$  was determined by the position of the source, i.e., the grid block  $\Delta\eta_1\Delta\xi$  was centered about the source, as shown in Figure 4.30a. The upper bound  $\bar{\eta}_1$  was then chosen using the same consideration of transport boundary conditions as that used in fixing the right-hand boundary  $x = \bar{x}_1$  for the Cartesian case. For the dimensionless streamline coordinate  $\xi$ , the upper bound  $\xi = \pi$  are fixed at the line of symmetry. The lower bound  $\xi = \bar{\xi}_0$  then was chosen by considering the largest streamline travel time which might contribute significantly to the radionuclide breakthrough at the target line  $\eta = 0$ .

Should this be 4.30b?

Should be  $x = 0$



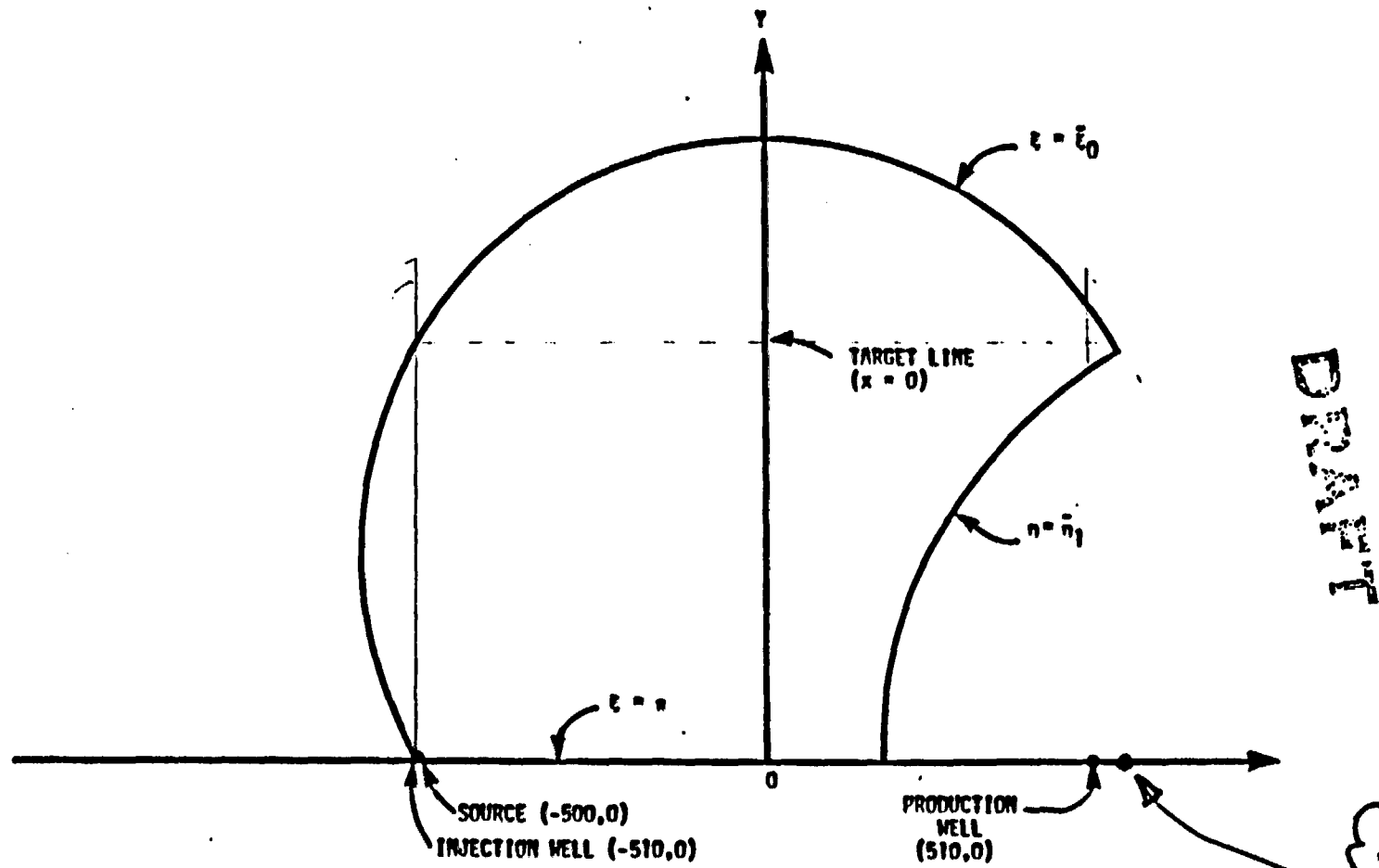


Figure 4.30a. Curvilinear coordinate geometry of flow region used in SHIFT for problem 8.2.

To simulate the flow system, the specified injection strength  $Q$  was partitioned among the individual streamtubes via  $Q\Delta\xi_j/2\pi$ . These injection rates were then applied at the boundary  $\eta = \bar{\eta}_0$ . To remove these flows, equal rates were then applied at the boundary  $\eta = \bar{\eta}_1$ . Since theoretically there can be no lateral flow across streamtube boundaries, no-flow conditions were prescribed along the boundaries  $\xi = \xi_0$  and  $\xi = \pi$ .

Spatially, the curvilinear system was discretized by the grid defined in Table 4.36. Darcy velocities from source to target line are maintained automatically at their analytic values in the curvilinear system. Thus, only two criteria were considered for the discretization. First, a spatial resolution of one percent or less was adopted for the source relative to the source-to-target distance. Secondly, the maximum length for a streamtube segment

$$\Delta s_{qij} \leq 4\alpha_L$$

was selected, where

$\Delta s_{qij}$  = length of grid block  $(i,j)$  in the  $\eta$  direction along its central streamline  $\xi$  ( $L$ )

$\alpha_L$  = longitudinal dispersivity ( $L$ )

A factor-of-two violation of the centered-in-space (CIS) (i.e., Peclet number) criterion (Lantz, 1971; Reeves et al., 1986b) was therefore permitted for the outermost streamtube  $\Delta\xi_1$  in the vicinity of the target line  $\eta = 0$ .

In fixing the  $\Delta\xi$  discretization, the resolution of the expected breakthrough profile was considered just as in the case of the Cartesian grid. Here, however, it was unnecessary to consider an additional refinement in the vicinity of the injection well since this is done automatically in curvilinear coordinates. Due to the fact that the chosen curvilinear coordinates are specially adapted to the two-well flow field, only  $17 \times 8$  (136) grid blocks were required as compared to  $50 \times 18$  (900) grid blocks for the Cartesian grid.

Should be  $x=0$

(4.9-5)

Should be  
(4.28)

Table 4.38. Pore volumes used in SWIFT for problem 8.2.

**DRAFT**

n - Index	Pore Volume* (m <sup>3</sup> )							
	E - Index							
	1	2	3	4	5	6	7	8
1	.0683	.0793	.101	.123	.144	.175	.212	.251
2	.188	.218	.277	.333	.388	.468	.565	.655
3	.522	.600	.758	.905	1.04	1.24	1.48	1.73
4	1.46	1.67	2.08	2.45	2.77	3.25	3.80	4.39
5	4.19	4.70	5.74	6.59	7.24	8.25	9.40	10.7
6	12.1	13.2	15.6	17.2	18.1	19.7	21.6	23.8
7	22.6	23.8	26.9	28.2	28.2	29.2	30.6	32.9
8	38.2	38.4	41.4	41.1	39.0	38.5	38.7	40.6
9	60.6	57.9	59.2	55.7	50.1	47.2	45.9	47.1
10	90.6	82.1	79.5	71.0	60.9	55.2	52.0	52.4
11	128.	110.	101.	85.9	70.8	62.0	57.0	56.8
12	166.	136.	120.	98.1	78.2	66.9	60.4	59.6
13	196.	156.	133.	107.	83.4	70.2	62.8	61.5
14	172.	135.	115.	91.2	70.9	59.5	53.0	51.8
15	196.	156.	133.	107.	83.4	70.2	62.8	61.5
16	166.	136.	120.	98.1	78.2	66.9	60.4	59.6
17	128.	110.	101.	85.9	70.8	62.0	57.0	56.8

\* See Equation (4.6-4) for a definition of pore volume in curvilinear coordinates.

Should be 4.14

DRAFT

Table 4.39. Darcy velocity throughout area modifiers used in SWIFT for problem 8.2.

n - Index	Darcy Velocity Throughput-Area Mod. for * ( $\times 10^3 \text{ m}^{-2}$ )							
	E- Index							
	1	2	3	4	5	6	7	8
1	123.00	123.00	124.00	124.00	124.00	125.00	126.00	126.00
2	74.30	74.60	74.90	75.30	75.70	76.20	76.80	77.10
3	44.70	45.00	45.30	45.70	46.10	46.70	47.20	47.50
4	26.80	27.00	27.30	27.70	28.20	28.70	29.20	29.60
5	15.90	16.20	16.50	16.90	17.30	17.90	18.40	18.70
6	9.38	9.62	9.92	10.30	10.80	11.30	11.80	12.20
7	5.48	5.71	6.01	6.40	6.87	7.39	7.91	8.27
8	3.64	3.87	4.18	4.57	5.03	5.55	6.07	6.44
9	2.61	2.85	3.15	3.54	4.00	4.52	5.04	5.41
10	1.98	2.21	2.51	2.90	3.37	3.89	4.41	4.77
11	1.57	1.80	2.10	2.49	2.96	3.48	4.00	4.36
12	1.30	1.54	1.84	2.23	2.70	3.22	3.74	4.10
13	1.15	1.38	1.60	2.08	2.54	3.06	3.58	3.95
14	1.08	1.31	1.61	2.01	2.47	2.99	3.51	3.87
15	1.08	1.31	1.61	2.01	2.47	2.99	3.51	3.87
16	1.15	1.38	1.69	2.08	2.54	3.06	3.58	3.95
17	1.30	1.54	1.84	2.23	2.70	3.22	3.74	4.10

\* See Equation (4.6-10) for a definition of the Darcy velocity throughput-area modifier.

This equation not in previous text. Should be Eq. 4.21?

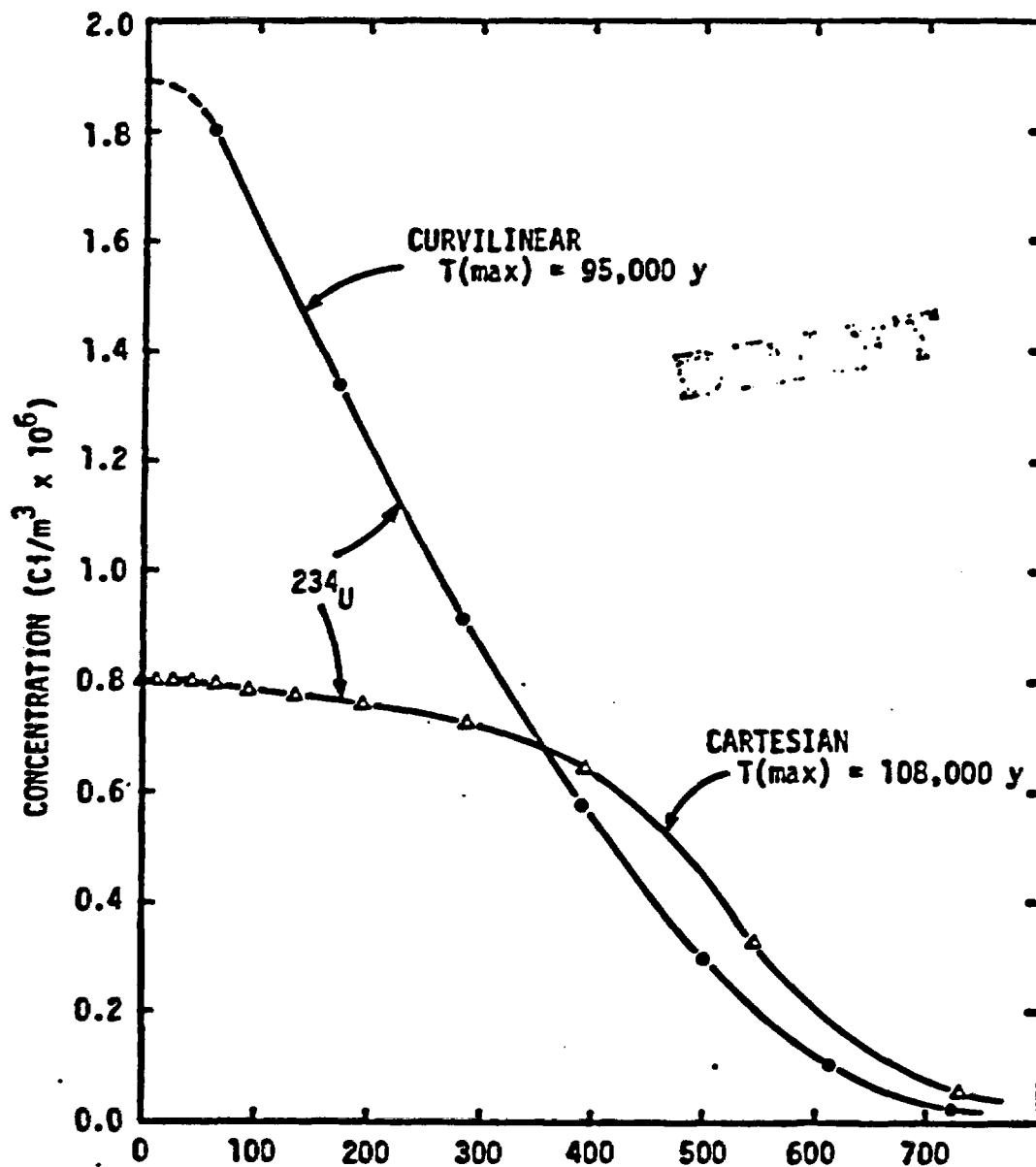


Figure 4.31. Target-line profiles of  $^{234}\text{U}$  at times of maximum discharge for Cartesian and curvilinear simulations of problem 8.2 using SWIFT.

4.40 \*

Table 4.9-7. Breakthrough Summary.

(a) Cartesian Simulation.

DRAFT

INTRACON

BENCHMARK CASE : 48

CODE : SWIFT-II

PARAMETERS : I1,R2,B2,P2,T2,E1,L1

NUCLIDE	C-MAX (CI/YR)	T-MAX (YEAR)	T+ (50%) (YEAR)	T- (50%) (YEAR)
1 U 234	4.1443E-06	108501.	39607.	148451.
2 TH 230	3.1137E-07	150000.	80343.	294373.
3 RA 226	8.9890E-06	139999.	75383.	271000.

NUCLIDE	C-MAX (CI/CU.M)	T-MAX (YEAR)	T+ (50%) (YEAR)	T- (50%) (YEAR)
1 U 234	8.0051E-07	108501.	39607.	148451.
2 TH 230	6.7891E-08	150000.	80343.	294373.
3 RA 226	2.1820E-06	139999.	75383.	271000.

(CONCENTRATION AT X = 0.0 M ; Y = 5.0 M)

Table 4.9-7. Breakthrough Summary.

4.40

(b) Curvilinear Simulation.

DRAFT

INTRACON

BENCHMARK CASE : 4B

CODE : SWIFT-II

PARAMETERS : I1,R2,B2,P2,T2,E1,L1

NUCLIDE	C-MAX (CI/YR)	T-MAX (YEAR)	T+ (50%) (YEAR)	T- (50%) (YEAR)
1 U 234	6.6023E-06	94999.	34322.	138409.
2 TH 230	5.0531E-07	139999.	74501.	276637.
3 RA 226	1.5181E-05	133330.	70662.	249510.

NUCLIDE	C-MAX (CI/CU.M)	T-MAX (YEAR)	T+ (50%) (YEAR)	T- (50%) (YEAR)
1 U 234	1.8030E-06	94999.	34322.	138409.
2 TH 230	1.4381E-07	139999.	74501.	276637.
3 RA 226	4.5713E-06	133330.	70662.	249510.

(CONCENTRATION AT X = 0.0 M ; Y = 5.0 M)

Table 4.9-8. Breakthrough Tabulations for the Cartesian Simulation.

INTRACON

BENCHMARK CASE : 4B

CODE : SWIFT-II

PARAMETERS : 11,R2,B2,P2,T2,E1,L1

TIME (YEARS)	NUCLIDE FLUX RATE (CI/YR)		
	U 234	TH 230	RA 226
3.17E-08	0.	0.	0.
5.00E+00	1.2570E-37	7.7142E-43	1.7130E-33
2.00E+01	6.5446E-31	1.2048E-35	2.7626E-27
3.50E+01	8.9756E-30	1.7728E-34	3.4663E-26
5.00E+01	6.5975E-29	1.3918E-33	2.3422E-25
1.00E+02	5.5647E-24	3.4138E-28	4.6871E-21
1.50E+02	6.4393E-23	4.2914E-27	4.6980E-20
2.00E+02	4.0700E-22	2.9257E-26	2.5984E-19
2.50E+02	1.8557E-21	1.4308E-25	1.0447E-18
5.00E+02	2.1476E-16	6.5764E-20	8.5141E-15
7.50E+02	2.0318E-15	6.8776E-19	6.1875E-14
1.00E+03	1.0596E-14	3.9307E-18	2.5380E-13
1.50E+03	6.9770E-14	2.8546E-17	1.2882E-12
2.00E+03	3.4448E-13	1.5539E-16	4.8893E-12
2.50E+03	1.3645E-12	6.7847E-16	1.4892E-11
3.00E+03	4.5311E-12	2.4824E-15	3.8168E-11
3.50E+03	1.3017E-11	7.8495E-15	8.5228E-11
4.00E+03	3.3128E-11	2.1956E-14	1.7028E-10
5.50E+03	4.0137E-10	4.2035E-13	8.8643E-10
7.00E+03	1.9392E-09	2.5622E-12	2.6912E-09
8.50E+03	6.2934E-09	1.0080E-11	6.2010E-09
1.00E+04	1.5899E-08	3.0298E-11	1.2022E-08
1.25E+04	5.1844E-08	1.3295E-10	2.8548E-08
1.50E+04	1.2127E-07	3.9396E-10	5.5603E-08
1.75E+04	2.3023E-07	9.2092E-10	9.5500E-08
2.00E+04	3.7827E-07	1.8274E-09	1.5017E-07
2.25E+04	5.5977E-07	3.2148E-09	2.2101E-07
2.50E+04	7.6634E-07	5.1609E-09	3.0879E-07
2.75E+04	9.8897E-07	7.7150E-09	4.1373E-07
3.00E+04	1.2194E-06	1.0899E-08	5.3553E-07
3.25E+04	1.4508E-06	1.4710E-08	6.7353E-07
3.50E+04	1.6778E-06	1.9128E-08	8.2677E-07
3.75E+04	1.8967E-06	2.4120E-08	9.9414E-07
4.00E+04	2.1048E-06	2.9643E-08	1.1744E-06
4.50E+04	2.4828E-06	4.2150E-08	1.5694E-06
5.00E+04	2.8081E-06	5.6199E-08	2.0027E-06
5.50E+04	3.0823E-06	7.1406E-08	2.4643E-06
6.00E+04	3.3103E-06	8.7424E-08	2.9463E-06
6.50E+04	3.4982E-06	1.0396E-07	3.4421E-06
7.00E+04	3.6519E-06	1.2078E-07	3.9466E-06



BENCHMARK CASE : 4B

CODE : SWIFT-11

PARAMETERS : 11,R2,B2,P2,T2,E1,L1

TIME (YEARS)	NUCLIDE FLUX RATE (CI/YR)		
	U 234	TH 230	RA 226
7.50E+04	3.7767E-06	1.3769E-07	4.4554E-06
8.00E+04	3.8775E-06	1.5455E-07	4.9649E-06
8.50E+04	3.9580E-06	1.7122E-07	5.4724E-06
9.00E+04	4.0215E-06	1.8764E-07	5.9757E-06
9.50E+04	4.0707E-06	2.0374E-07	6.4731E-06
1.00E+05	4.1078E-06	2.1948E-07	6.9632E-06
1.00E+05	4.1078E-06	2.1949E-07	6.9638E-06
1.00E+05	4.1079E-06	2.1954E-07	6.9652E-06
1.00E+05	4.1080E-06	2.1958E-07	6.9667E-06
1.00E+05	4.1081E-06	2.1963E-07	6.9681E-06
1.00E+05	4.1084E-06	2.1978E-07	6.9730E-06
1.00E+05	4.1088E-06	2.1993E-07	6.9779E-06
1.00E+05	4.1091E-06	2.2008E-07	6.9827E-06
1.00E+05	4.1094E-06	2.2024E-07	6.9875E-06
1.01E+05	4.1110E-06	2.2100E-07	7.0117E-06
1.01E+05	4.1125E-06	2.2175E-07	7.0359E-06
1.01E+05	4.1140E-06	2.2251E-07	7.0600E-06
1.01E+05	4.1170E-06	2.2403E-07	7.1080E-06
1.02E+05	4.1199E-06	2.2554E-07	7.1557E-06
1.02E+05	4.1227E-06	2.2705E-07	7.2029E-06
1.03E+05	4.1253E-06	2.2856E-07	7.2494E-06
1.04E+05	4.1280E-06	2.3006E-07	7.2950E-06
1.04E+05	4.1305E-06	2.3155E-07	7.3393E-06
1.05E+05	4.1371E-06	2.3604E-07	7.4655E-06
1.07E+05	4.1422E-06	2.4049E-07	7.5830E-06
1.09E+05	4.1443E-06	2.4490E-07	7.6948E-06
1.10E+05	4.1418E-06	2.4926E-07	7.8031E-06
1.13E+05	4.1211E-06	2.5643E-07	7.9768E-06
1.15E+05	4.0735E-06	2.6337E-07	8.1408E-06
1.18E+05	3.9944E-06	2.7001E-07	8.2927E-06
1.20E+05	3.8844E-06	2.7627E-07	8.4308E-06
1.23E+05	3.7478E-06	2.8205E-07	8.5540E-06
1.25E+05	3.5910E-06	2.8732E-07	8.6616E-06
1.27E+05	3.4210E-06	2.9203E-07	8.7535E-06
1.30E+05	3.2439E-06	2.9615E-07	8.8296E-06
1.32E+05	3.0650E-06	2.9971E-07	8.8904E-06
1.35E+05	2.8884E-06	3.0271E-07	8.9367E-06
1.38E+05	2.7171E-06	3.0517E-07	8.9693E-06
1.40E+05	2.5531E-06	3.0714E-07	8.9890E-06
1.50E+05	1.9840E-06	3.1137E-07	8.9683E-06

-----  
BENCHMARK CASE : 4B

CODE : SWIFT-11

PARAMETERS : I1,R2,B2,P2,T2,E1,L1  
-----

TIME (YEARS)	NUCLIDE FLUX RATE (CI/YR)		
	U 234	TH 230	RA 226
1.60E+05	1.5544E-06	3.1015E-07	8.8094E-06
1.70E+05	1.2408E-06	3.0526E-07	8.5478E-06
1.80E+05	1.0106E-06	2.9792E-07	8.2187E-06
1.90E+05	8.3804E-07	2.8883E-07	7.8431E-06
2.00E+05	7.0580E-07	2.7841E-07	7.4378E-06
2.10E+05	6.0223E-07	2.6693E-07	7.0145E-06
2.20E+05	5.1949E-07	2.5460E-07	6.5832E-06
2.30E+05	4.5219E-07	2.4161E-07	6.1517E-06
2.40E+05	3.9662E-07	2.2817E-07	5.7264E-06
2.50E+05	3.5294E-07	2.1451E-07	5.3122E-06
2.60E+05	3.1501E-07	2.0082E-07	4.9126E-06
2.70E+05	2.8164E-07	1.8726E-07	4.5308E-06
2.80E+05	2.5242E-07	1.7398E-07	4.1683E-06
2.90E+05	2.2688E-07	1.6110E-07	3.8268E-06
3.00E+05	2.0453E-07	1.4873E-07	3.5071E-06

-----

4.42

Table 4.8-9. Breakthrough Tabulations for the Curvilinear Simulation.

BENCHMARK CASE : 4B

CODE : SWIFT-11

PARAMETERS : 11,R2,B2,P2,T2,E1,L1

TIME (YEARS)	NUCLIDE FLUX RATE (CI/YR)		
	U 234	TH 230	RA 226
0.	0.	0.	0.
1.00E+02	5.5731E-20	6.8346E-24	6.6167E-18
2.00E+02	6.2466E-19	8.3433E-23	6.4037E-17
3.00E+02	3.7824E-18	5.4722E-22	3.3681E-16
4.00E+02	1.6412E-17	2.5595E-21	1.2762E-15
5.00E+02	5.7144E-17	9.5651E-21	3.8990E-15
1.00E+03	9.7880E-15	3.0275E-18	2.3072E-13
2.00E+03	2.5450E-12	1.5677E-15	1.5897E-11
3.00E+03	2.7554E-11	1.9986E-14	1.1577E-10
4.00E+03	1.5902E-10	1.3406E-13	4.7116E-10
5.00E+03	6.3691E-10	6.2021E-13	1.3724E-09
7.50E+03	9.4363E-09	1.5980E-11	9.0054E-09
1.00E+04	4.3917E-08	9.7031E-11	2.8666E-08
1.25E+04	1.2951E-07	3.5940E-10	6.6126E-08
1.50E+04	2.8899E-07	9.8948E-10	1.2649E-07
1.75E+04	5.3247E-07	2.2193E-09	2.1417E-07
2.00E+04	8.5485E-07	4.2832E-09	3.3265E-07
2.33E+04	1.3765E-06	8.6774E-09	5.4219E-07
2.67E+04	1.9601E-06	1.5175E-08	8.1158E-07
3.00E+04	2.5598E-06	2.3868E-08	1.1385E-06
3.33E+04	3.1409E-06	3.4680E-08	1.5182E-06
3.67E+04	3.6809E-06	4.7423E-08	1.9443E-06
4.00E+04	4.1678E-06	6.1846E-08	2.4102E-06
4.50E+04	4.7904E-06	8.6091E-08	3.1696E-06
5.00E+04	5.2886E-06	1.1259E-07	3.9844E-06
5.50E+04	5.6759E-06	1.4055E-07	4.8350E-06
6.00E+04	5.9703E-06	1.6928E-07	5.7071E-06
6.50E+04	6.1891E-06	1.9826E-07	6.5898E-06
7.00E+04	6.3477E-06	2.2709E-07	7.4741E-06
7.50E+04	6.4588E-06	2.5549E-07	8.3538E-06
8.00E+04	6.5324E-06	2.8326E-07	9.2244E-06
8.50E+04	6.5770E-06	3.1028E-07	1.0082E-05
9.00E+04	6.5986E-06	3.3645E-07	1.0926E-05
9.50E+04	6.6023E-06	3.6176E-07	1.1752E-05
1.00E+05	6.5917E-06	3.8620E-07	1.2562E-05
1.00E+05	6.5913E-06	3.8666E-07	1.2578E-05
1.00E+05	6.5909E-06	3.8713E-07	1.2594E-05
1.00E+05	6.5906E-06	3.8760E-07	1.2610E-05
1.00E+05	6.5903E-06	3.8807E-07	1.2625E-05
1.01E+05	6.5899E-06	3.8855E-07	1.2642E-05

-----  
BENCHMARK CASE : 4B

CODE : SWIFT-II

PARAMETERS : 11,R2,B2,P2,T2,E1,L1  
-----

TIME (YEARS)	NUCLIDE FLUX RATE (CI/YR)		
	U 234	TH 230	RA 226
1.01E+05	6.5883E-06	3.9088E-07	1.2721E-05
1.02E+05	6.5844E-06	3.9554E-07	1.2878E-05
1.03E+05	6.5802E-06	4.0017E-07	1.3030E-05
1.04E+05	6.5755E-06	4.0478E-07	1.3174E-05
1.05E+05	6.5701E-06	4.0934E-07	1.3307E-05
1.07E+05	6.5494E-06	4.2069E-07	1.3604E-05
1.10E+05	6.5073E-06	4.3177E-07	1.3871E-05
1.13E+05	6.4248E-06	4.4252E-07	1.4122E-05
1.15E+05	6.2852E-06	4.5281E-07	1.4353E-05
1.18E+05	6.0809E-06	4.6246E-07	1.4558E-05
1.20E+05	5.8159E-06	4.7130E-07	1.4735E-05
1.23E+05	5.3913E-06	4.8161E-07	1.4925E-05
1.27E+05	4.9184E-06	4.9005E-07	1.5062E-05
1.30E+05	4.4317E-06	4.9653E-07	1.5146E-05
1.33E+05	3.9576E-06	5.0114E-07	1.5181E-05
1.37E+05	3.5132E-06	5.0400E-07	1.5172E-05
1.40E+05	3.1077E-06	5.0531E-07	1.5123E-05
1.50E+05	2.1355E-06	5.0288E-07	1.4803E-05
1.60E+05	1.4879E-06	4.9281E-07	1.4280E-05
1.70E+05	1.0728E-06	4.7853E-07	1.3629E-05
1.80E+05	8.0418E-07	4.6190E-07	1.2904E-05
1.90E+05	6.2475E-07	4.4373E-07	1.2137E-05
2.00E+05	5.0000E-07	4.2428E-07	1.1348E-05
2.20E+05	3.3799E-07	3.8237E-07	9.7733E-06
2.40E+05	2.4308E-07	3.3703E-07	8.2566E-06
2.60E+05	1.7998E-07	2.9042E-07	6.8562E-06
2.80E+05	1.3474E-07	2.4502E-07	5.6119E-06
3.00E+05	1.0085E-07	2.0294E-07	4.5380E-06

-----

4.43

Table 4.9-10. Target-Line Distribution of  $^{234}\text{U}$  at  $T(\text{MAX}) = 108,500$  y for the Cartesian Simulation.

INTRA COIN

BENCHMARK CASE : 4B

CODE : SWIFT-II

PARAMETERS : I1,R2,B2,P2,T2,E1,L1

T-MAX = 108501. YEARS

NUCLIDE	Y-ORDINATE (M)	CONCENTRATION (CI/CU.M)
U 234	.5	8.0056E-07
	2.0	8.0056E-07
	4.0	8.0053E-07
	7.0	8.0046E-07
	12.0	8.0028E-07
	19.0	7.9981E-07
	29.0	7.9881E-07
	44.0	7.9662E-07
	65.0	7.9240E-07
	95.0	7.8492E-07
	137.0	7.7351E-07
	197.0	7.5669E-07
	281.0	7.2926E-07
	395.0	6.4984E-07
	545.0	3.2977E-07
	731.0	5.8471E-08
	953.0	3.2611E-09
	1211.5	6.1794E-11

4.44

Table 4.9-11. Target-Line Distribution of  $^{230}\text{Th}$  at  $T(\text{MAX}) = 150,000$  y for the Cartesian Simulation.

BENCHMARK CASE : 4B

CODE : SWIFT-11

PARAMETERS : 11,R2,B2,P2,T2,E1,L1

T-MAX = 150000. YEARS

NUCLIDE	Y-ORDINATE (M)	CONCENTRATION (CI/CU.M)
TH 230	.5	6.7919E-08
	2.0	6.7915E-08
	4.0	6.7902E-08
	7.0	6.7869E-08
	12.0	6.7771E-08
	19.0	6.7547E-08
	29.0	6.7069E-08
	44.0	6.6051E-08
	65.0	6.4203E-08
	95.0	6.1334E-08
	137.0	5.7961E-08
	197.0	5.5069E-08
	281.0	5.2428E-08
	395.0	4.4803E-08
	545.0	2.4450E-08
	731.0	5.5712E-09
	953.0	4.3785E-10
	1211.5	1.2052E-11

4.45  
 Table 4.9-12. Target-Line Distribution of  $^{226}\text{Ra}$  at  $T(\text{MAX}) = 140,000$  y  
 for the Cartesian Simulation.

BENCHMARK CASE : 4B

CODE : SWIFT-II

PARAMETERS : I1,R2,B2,P2,T2,E1,L1

T-MAX = 139999. YEARS

NUCLIDE	Y-ORDINATE (M)	CONCENTRATION (CI/CU.M)
RA 226	.5	2.1827E-06
	2.0	2.1826E-06
	4.0	2.1822E-06
	7.0	2.1814E-06
	12.0	2.1788E-06
	19.0	2.1729E-06
	29.0	2.1600E-06
	44.0	2.1319E-06
	65.0	2.0771E-06
	95.0	1.9800E-06
	137.0	1.8317E-06
	197.0	1.6364E-06
	281.0	1.4194E-06
	395.0	1.1205E-06
	545.0	5.7376E-07
	731.0	1.2283E-07
	953.0	9.0965E-09
	1211.5	2.3717E-10

4.46

Table 4.9-13. Target-Line Distribution of  $^{234}\text{U}$  at  $T(\text{MAX}) = 95,000$  y for the Curvilinear Simulation.

BENCHMARK CASE : 4B

CODE : SWIFT-II

PARAMETERS : I1,R2,B2,P2,T2,E1,L1

T-MAX = 94999. YEARS

NUCLIDE	Y-ORDINATE (M)	CONCENTRATION (CI/CU.M)
U 234	831.8	4.9990E-09
	722.0	2.4616E-08
	611.7	1.0355E-07
	500.3	3.0020E-07
	392.4	5.7992E-07
	285.8	9.1025E-07
	176.1	1.3410E-06
	60.0	1.8076E-06



4.47

Table 4.9-14: Target-Line Distribution of  $^{230}\text{Th}$  at  $T(\text{MAX}) = 140,000$  y for the Curvilinear Simulation.

BENCHMARK CASE : 4B

CODE : SWIFT-II

PARAMETERS : I1,R2,B2,P2,T2,E1,L1

T-MAX = 139999. YEARS

NUCLIDE	Y-ORDINATE (M)	CONCENTRATION (CI/CU.M)
TH 230	831.8	7.9534E-10
	722.0	3.0377E-09
	611.7	9.6319E-09
	500.3	2.2493E-08
	392.4	4.0730E-08
	285.8	6.5202E-08
	176.1	1.0061E-07
	60.0	1.4424E-07

DRAFT

4.48

Table 4.9-15. Target-Line Distribution of  $^{226}\text{Ra}$  at  $T(\text{MAX}) = 133,330$  y for the Curvilinear Simulation.

BENCHMARK CASE : 4B

CODE : SWIFT-II

PARAMETERS : I1,R2,B2,P2,T2,E1,L1

T-MAX = 133330. YEARS

NUCLIDE	Y-ORDINATE (M)	CONCENTRATION (CI/CU.M)
RA 226	831.8	1.9046E-08
	722.0	7.3441E-08
	611.7	2.3629E-07
	500.3	5.6347E-07
	392.4	1.0567E-06
	285.8	1.8098E-06
	176.1	3.0477E-06
	60.0	4.5867E-06

#### 4.10 PROBLEM 8.4: TRANSPORT OF A THREE-MEMBER CHAIN OF RADIONUCLIDES FROM A HYPOTHETICAL BASALT REPOSITORY

##### 4.10.1 Problem Statement and Objectives

The physical system is the same as that of problem 3.5. Insofar as the flow is concerned, there are several important units of the system, all of which are shown in Figures 2.14 through 2.16. They include two aquifers separated by an aquitard, zones of recharge and high permeability caused by the uplift of ridges, an ancient river bed and a river. All of these features influence the flow within the entire basalt basin.

Within this hypothetical system, a repository is located as shown in Figures 4.18 and 4.19. The heat generated influences the flow field, particularly within the immediate vicinity of the repository. As discussed in Section 4.7, the presence of the heat significantly enhances the upwardly directed Darcy velocities passing through the repository. Based on simulations extending beyond 10,000 years, it was found that these velocities return effectively to their isothermal values after 725,000 years.

The objective of this problem is to follow the movement of a three-member actinide chain as it is transported from repository to river by the nonisothermal, transient flow field. The desired output is the breakthrough of each species at the river.

##### 4.10.2 Input Specifications

Porosities are given in Table 4.2 and radionuclide-dependent data are given in Table 4.49. Dispersivity values are given in Table 4.50. The flow field, of course, is obtained from the output of problems 5.3 (Section 4.7) and 3.5 (Section 4.4).

##### 4.10.3 Input Modifications and Discretization Data

In examining the isothermal flow field obtained for the latter problem, the streamline passing through the repository was obtained (see Streamline E of Figure 4.8 and 4.9). Several multidimensional effects were then evaluated relative to this path, which is denoted here as the basic streamline. First, streamlines passing through the

2.16


2.18

4.50

Would greatly facilitate reading the text if these figures were duplicated and inserted within the section.


Table 4.50. Dispersivity and porosity values used in SWIFT for problem 8.4.

DRAFT



Leg*	Rock Type	Dispersivity (m)	Porosity
A	Basalt	100	0.01
B	Aquifer 1	100	0.20
C	Crushed Zone	10	0.30
D	Crushed Zone	10	0.30
E	Crushed Zone	10	0.30
F	Crushed Zone	10	0.30
G	Crushed Zone	10	0.30
H	Ancient River Bed	20	0.30
I	Aquifer 1	100	0.20

\* For definition of leg A through I, see Fig 4.32



Add this note  
to this table

This reference is not correct.

four corners of the repository were obtained, and travel times from repository to river were evaluated. The smearing resulting from this effect was found to be negligible in comparison to the longitudinal dispersion prescribed in Table 4.10. Secondly, transverse dispersion, assumed to be 10 percent of longitudinal dispersion, was examined. Since the river serves as a lateral integrator for the breakthrough, there was concern that material would be dispersed laterally to a streamline with a substantially different travel time from that of the basic path. Thus lateral dispersion is negligible. Thirdly, and finally, dimensional effects arising from the thermal plume (see Figure 4.22) were also considered. These appeared to be negligible. Thus the radionuclide transport was assumed to be one-dimensional following the basic streamline of the repository center.

The one-dimensional system adopted for this simulation is shown in Figure 4.32. As indicated, it consists of nine separate legs, one for each velocity zone within the basic streamline. To establish the desired interstitial velocities within the upper aquifer, an injection well is used, and the cross-sectional areas of the various legs are adjusted. Table 4.51 provides the details. To establish the flow within the aquitard, an injection well is also used. Here, however, in order to characterize thermal effects, the velocity is varied in accordance with the "average" curve generated for problem 5.3 (see Figure 4.24). Table 4.52 provides the injection schedule. A constant pressure ( $p = 0$ ) is imposed at the river boundary, and the individual legs are gridded as shown in Table 4.53.

#### 4.10.4 Simulation Results

Two breakthrough curves were determined, one for the nonisothermal case and, for comparison, one for the isothermal case. For the latter the Darcy velocity in the aquitard was fixed at  $u_z = 2.78 \times 10^{-6}$  m/yr. Otherwise the two simulations were identical. The two breakthrough curves are summarized in Table 4.54 and tabulated in Table 4.55 and 4.56. The heat source produces an earlier breakthrough (by roughly 10 percent) and a reduced maximum (by roughly 10 percent).

WM DOCKET CONTROL  
CENTER

'87 SEP -9 A11:13

PDR-1  
LPDR WM-10(2)  
WM-11(2)  
WM-16(2)

WM-RES

WM Record File

DLG 85  
Corstar

WM Project 10, 11, 16

Docket No. \_\_\_\_\_

PDR ☒

LPDR ☒ (B, N, S)

Distribution:

PB/MS

(Return to WM, 623-SS)

4174